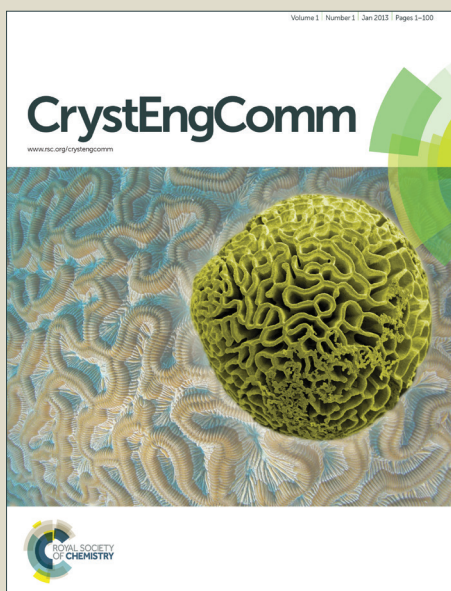


# CrystEngComm

Accepted Manuscript



This is an *Accepted Manuscript*, which has been through the Royal Society of Chemistry peer review process and has been accepted for publication.

*Accepted Manuscripts* are published online shortly after acceptance, before technical editing, formatting and proof reading. Using this free service, authors can make their results available to the community, in citable form, before we publish the edited article. We will replace this *Accepted Manuscript* with the edited and formatted *Advance Article* as soon as it is available.

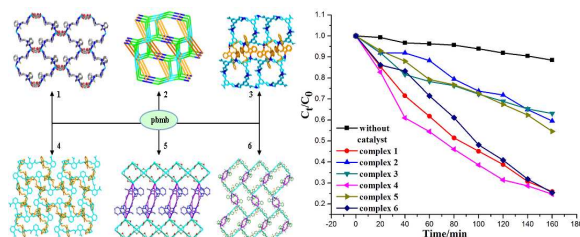
You can find more information about *Accepted Manuscripts* in the [Information for Authors](#).

Please note that technical editing may introduce minor changes to the text and/or graphics, which may alter content. The journal's standard [Terms & Conditions](#) and the [Ethical guidelines](#) still apply. In no event shall the Royal Society of Chemistry be held responsible for any errors or omissions in this *Accepted Manuscript* or any consequences arising from the use of any information it contains.

# Novel Coordination Polymers of Zn(II) and Cd(II) Tuned by Different Aromatic Polycarboxylates: Synthesis, Structures and Photocatalytic Properties

5 Ming Li, Lu Liu, Lin Zhang, Xiaofeng Lv, Jie Ding\*, Hongwei Hou\*, Yaoting Fan

Six fascinating coordination polymers (CPs) showed good photocatalytic activities for the degradation of methylene blue (MB).



10

15

20

Cite this: DOI: 10.1039/c0xx00000x

www.rsc.org/xxxxxx

ARTICLE TYPE

CrystEngComm Accepted Manuscript

# Novel Coordination Polymers of Zn(II) and Cd(II) Tuned by Different Aromatic Polycarboxylates: Synthesis, Structures and Photocatalytic Properties

Ming Li, Lu Liu, Lin Zhang, Xiaofeng Lv, Jie Ding\*, Hongwei Hou\*, Yaoting Fan

Received (in XXX, XXX) Xth XXXXXXXXXX 20XX, Accepted Xth XXXXXXXXXX 20XX

First published on the web Xth XXXXXXXXXX 20XX

DOI: 10.1039/b000000x

Tuned by different aromatic polycarboxylates, six fascinating coordination polymers (CPs), namely,  $[\text{Cd}(\text{pbmb})(p\text{-bdc})]_n$  (**1**),  $\{[\text{Zn}_3(\text{pbmb})_2(1,3,5\text{-btc})_2]\cdot 6\text{H}_2\text{O}\}_n$  (**2**),  $\{[\text{Cd}_3(\text{pbmb})_3(1,3,5\text{-btc})_2(\text{H}_2\text{O})]\cdot 3\text{H}_2\text{O}\}_n$  (**3**),  $\{[\text{Zn}_2(\text{pbmb})(1,2,3\text{-btc})(\mu_2\text{-OH})]\cdot \text{H}_2\text{O}\}_n$  (**4**),  $[\text{Cd}(\text{pbmb})(1,2,4,5\text{-btec})_{0.5}]_n$  (**5**),  $\{[\text{Cd}(\text{pbmb})(\text{sdba})]\cdot 2\text{H}_2\text{O}\}_n$  (**6**) (pbmb = 1,1'-(1,3-propane)bis-(2-methylbenzimidazole), *p*-H<sub>2</sub>bdc = 1,4-benzenedicarboxylic acid, 1,3,5-H<sub>3</sub>btc = 1,3,5-benzenetricarboxylic acid, 1,2,3-H<sub>3</sub>btc = 1,2,3-benzenetricarboxylic acid, 1,2,4,5-H<sub>4</sub>btec = 1,2,4,5-benzenetetracarboxylic acid, H<sub>2</sub>sdba = 4,4'-sulfonyldibenzoic acid), have been ideated and manufactured by the hydrothermal reaction methods. Structural analyses reveal that complexes **1–3** feature the three-dimensional (3D) structures (**1**: 4-connected 6<sup>6</sup> topology, **2**: (3, 4, 6)-connected (6<sup>5</sup>.7)(4.6<sup>2</sup>)<sub>2</sub>(4<sup>2</sup>.6<sup>6</sup>.8<sup>5</sup>.10<sup>2</sup>) topology and **3**: (2, 3, 4)-connected (6<sup>5</sup>.8)<sub>2</sub>(6<sup>3</sup>)<sub>2</sub> topology), and the rest of CPs **4–6** exhibit the 2D networks. The thermal stability and powder X-ray diffraction for **1–6** have been investigated for further properties. The optical band gaps are analyzed by diffuse-reflectance UV-vis spectra. Moreover, all of the materials manifest good photocatalytic activities for the degradation of methylene blue (MB) (**1**: 74 %, **2**: 41 %, **3**: 37 %, **4**: 76%, **5**: 46%, **6**: 75%, respectively) in water under the irradiation of high-pressure mercury lamp.

## Introduction

During the last two decades, rapidly expanding development in coordination polymers (CPs), especially metal-organic framework (MOF) materials, has motivated the chemists to achieve the diverse multifunctional applications in gas storage and separation,<sup>1</sup> heterogeneous catalysis,<sup>2</sup> molecular magnets,<sup>3</sup> electrical conduction<sup>4</sup> and luminescence materials.<sup>5</sup> Noteworthy, the design and construction of intriguing and useful CPs, influenced by different factors (metal ions, organic ligands, solvent system, PH value and reaction temperature, etc),<sup>6</sup> are also

tremendous challenges in the fields of coordination chemistry and crystal engineering. In the previous work of our group, based on a series of bis(methyl-benzimidazole) ligands with  $-(\text{CH}_2)_n-$  backbones, many marvellous architectures were successfully obtained.<sup>7</sup> Meanwhile, we found that the  $-(\text{CH}_2)_n-$  backbone and the 2-position substituent methyl group could strengthen the coordination ability of the ligands with metal ions.<sup>8-9</sup> Thereupon, by using the imidazole ligand as a versatile scaffold, a systematic research of the multidimensional CPs about the impact of different auxiliary aromatic polycarboxylates would be feasible and valuable.

On the other hand, photocatalysis, by the growing concern on human activities regarding the underlying adverse health effects, which can effectively degrade the contaminated organic dyes in wastewater without further contamination, is considered as a green ecological technology.<sup>10</sup> Currently, as emerging and energetic heterogeneous photocatalysts, some CPs materials are already used to degrade organic pollutants.<sup>11-13</sup> According to the photocatalytic mechanism of reported CPs material,<sup>11b, 14</sup> which behave as sensitive semiconductors, when electrons ( $e^-$ ) is excited

<sup>a</sup> The College of Chemistry and Molecular Engineering, Zhengzhou University, Zhengzhou 450001, P. R. China. E-mail: jieding@zzu.edu.cn, houthongw@zzu.edu.cn; Tell: (+86) 371-67761744

<sup>†</sup>Electronic supplementary information (ESI) available: X-ray crystallographic data, selected bond lengths and bond angles, additional crystal figures, powder X-ray patterns, TGA curves and the Kubelka-Munk-transformed diffuse reflectance for complexes **1–6**. CCDC reference numbers: 979662-979667 for **1–6**. For ESI and crystallographic data in CIF or other electronic format see DOI:10.1039/b000000x/

from its valence bond (VB) to the conduction band (CB) under the irradiation of UV-visible light, the same amount of holes ( $h^+$ ) will be retained in the VB. At the following step, such highly active electrons would quickly transfer to  $O_2$  adsorbed on the CPs to form the  $\cdot O_2^-$  radicals, which might transform to the hydroxyl radicals ( $\cdot OH$ ). At the same time, the hydroxyl ( $OH^-$ ) adsorbed on the CPs interaction with the hole ( $h^+$ ) retained in the VB can also generate hydroxyl radicals ( $\cdot OH$ ), resulting that the relative electrons return the VB of the CPs to accomplish the photocatalytic circulation. As well-known, the hydroxyl radicals ( $\cdot OH$ ) can degrade effectively the organic dye such as methylene blue (MB).<sup>15</sup> Actually, as an electron ( $e^-$ ) and hole ( $h^+$ ) transfer process driven by the light, the catalysis is controlled by several influences. The optical band gap ( $E_g$ ) and the sorption of  $O_2/OH^-$  on the CPs are two of the key factors, which are distinctly connected with the constructions of the CPs. Additionally, the supply of free  $O_2/OH^-$  in water also affects the photocatalytic procedure.

Inspired by the above ideas, we employed 1,1'-(1,3-propane)bis-(2-methylbenzimidazole) (pbmb) and five kinds of aromatic polycarboxylates to successfully obtain six novel coordination polymers, namely,  $[Cd(pbmb)(p-bdc)]_n$  (**1**),  $\{[Zn_3(pbmb)_2(1,3,5-btc)_2] \cdot 6H_2O\}_n$  (**2**),  $\{[Cd_3(pbmb)_3(1,3,5-btc)_2(H_2O)] \cdot 3H_2O\}_n$  (**3**),  $\{[Zn_2(pbmb)(1,2,3-btc)(\mu_2-OH)] \cdot H_2O\}_n$  (**4**),  $[Cd(pbmb)(1,2,4,5-btec)_{0.5}]_n$  (**5**),  $\{[Cd(pbmb)(sdba)] \cdot 2H_2O\}_n$  (**6**) ( $p$ -H<sub>2</sub>bdc = 1,4-benzenedicarboxylic acid, 1,3,5-H<sub>3</sub>btc = 1,3,5-benzenetricarboxylic acid, 1,2,3-H<sub>3</sub>btc = 1,2,3-benzenetricarboxylic acid, 1,2,4,5-H<sub>4</sub>btec = 1,2,4,5-benzenetetracarboxylic acid, H<sub>2</sub>sdba = 4,4'-sulfonyldibenzoic acid), which showed widely different structures and topologies determined by single-crystal X-ray diffraction analyses and further characterized by infrared spectra (IR), elemental analyses, powder X-ray diffraction (PXRD), and thermogravimetric (TG) analyses. The optical band gaps of CPs **1–6** were analyzed by diffuse-reflectance UV-vis absorption spectra. Moreover, all of the materials showed good photocatalytic activities for the degradation of methylene blue (MB) (**1**: 74 %, **2**: 41 %, **3**: 37 %, **4**: 76%, **5**: 46%, **6**: 75%, respectively) in water under high-pressure mercury lamp irradiation.

## 40 Experimental section

**Materials and Physical Measurements.** The pbmb ligand was synthesized in accordance with the literature,<sup>16</sup> while the other reagents and solvents employed were commercially available and used as received without any further purification. The FT-IR spectra were recorded in the range of 400–4000  $cm^{-1}$  on a Bruker Tensor 27 spectrophotometer from KBr pellets. Elemental analyses (C, N, S and H) were carried out on a FLASH EA 1112 elemental analyzer. PXRD Patterns were performed using Cu K $\alpha$ 1 radiation on a PANalytical X'Pert PRO diffractometer. Thermal analyses (TGA) were obtained on a Netzsch STA 449C thermal analyzer from room temperature at a heating rate of 10  $^\circ C min^{-1}$  in air.

### Synthesis

**Synthesis of  $[Cd(pbmb)(p-bdc)]_n$  (**1**).** A suspension of  $Cd(NO_3)_2 \cdot 4H_2O$  (30.8 mg, 0.1 mmol), pbmb (30.4 mg, 0.1 mmol),  $p$ -H<sub>2</sub>bdc (16.6 mg, 0.1 mmol), and NaOH (8.0 mg, 0.2

mmol) in 10mL of distilled H<sub>2</sub>O was sealed in a 25 mL Teflon-lined stainless steel container and heated at 130  $^\circ C$  for 3 days. After the mixture was cooled to ambient temperature at a rate of 5  $^\circ C h^{-1}$ , colorless block crystals of **1** were obtained with a yield of 70 % (based on Cd). Anal. calcd for  $C_{27}H_{24}N_4O_4Cd$  (%): C, 55.82; H, 4.16; N, 9.64. Found: C, 55.53; H, 4.17; N, 9.34. IR (KBr,  $cm^{-1}$ ): 3432(w), 3108(w), 1569(m), 1506(m), 1454(m), 1438(m), 1392(s), 1287(m), 1229(m), 1160(m), 1012(m), 839(s), 752(s), 666(w), 531(m).

**Synthesis of  $\{[Zn_3(pbmb)_2(1,3,5-btc)_2] \cdot 6H_2O\}_n$  (**2**).** Complex **2** was obtained by the similar synthetic procedure of **1** with a yield of 38 % (based on Zn). Anal. calcd for  $C_{56}H_{58}N_8O_{18}Zn_3$  (%): C, 50.67; H, 4.40; N, 8.44. Found: C, 50.95; H, 4.05; N, 8.30. IR (KBr,  $cm^{-1}$ ): 3433(w), 3132(w), 1624(m), 1580(m), 1436(m), 1408(m), 1360(s), 1167(m), 1105(m), 1021(m), 938(m), 741(s), 562(m), 460(m).

**Synthesis of  $\{[Cd_3(pbmb)_3(1,3,5-btc)_2(H_2O)] \cdot 3H_2O\}_n$  (**3**).** The same synthetic method as that of **2** was used except that  $Zn(NO_3)_2 \cdot 6H_2O$  was replaced by  $Cd(NO_3)_2 \cdot 4H_2O$  (30.8 mg, 0.1 mmol). The yield of crystal **3** was 85 % (based on Cd). Anal. calcd for  $C_{75}H_{74}N_{12}O_{16}Cd_3$  (%): C, 51.87; H, 4.29; N, 9.68. Found: C, 52.16; H, 4.41; N, 9.37. IR (KBr,  $cm^{-1}$ ): 3422(w), 3127(w), 1611(m), 1555(m), 1433(m), 1407(m), 1367(s), 1290(m), 1248(m), 1164(m), 1101(m), 1012(m), 932(m), 873(w), 844(w), 741(s), 527(w), 431(w).

**Synthesis of  $\{[Zn_2(pbmb)(1,2,3-btc)(\mu_2-OH)] \cdot H_2O\}_n$  (**4**).** A suspension of 1,2,3-H<sub>3</sub>btc (21.0 mg, 0.1 mmol),  $Zn(NO_3)_2 \cdot 6H_2O$  (29.7 mg, 0.1 mmol), ethyl alcohol (5.0 mL), and H<sub>2</sub>O (5.0 mL) was sealed in a 25 mL Teflon-lined stainless steel container, heated to 130  $^\circ C$  for 3 days. After the mixture was cooled to ambient temperature at a rate of 5  $^\circ C h^{-1}$ , colorless block crystals of **4** were achieved with a yield of 80 % (based on Zn). Anal. calcd for  $C_{28}H_{26}N_4O_8Zn_2$  (%): C, 49.65; H, 3.87; N, 8.27. Found: C, 49.86; H, 3.84; N, 7.95. IR (KBr,  $cm^{-1}$ ): 3639(w), 3363(m), 3236(w), 3136(w), 2933(m), 1615(m), 1596(m), 1514(m), 1463(m), 1410(w), 1359(s), 1166(w), 1065(w), 1016(m), 938(m), 848(m), 811(s), 755(s), 703(m), 496(m).

**Synthesis of  $[Cd(pbmb)(1,2,4,5-btec)_{0.5}]_n$  (**5**).** A suspension of  $Cd(NO_3)_2 \cdot 4H_2O$  (30.8 mg, 0.1 mmol), pbmb (30.4 mg, 0.1 mmol), 1,2,4,5-H<sub>4</sub>btec (25.4 mg, 0.1 mmol), and NaOH (16.0 mg, 0.4 mmol) in 10mL of distilled H<sub>2</sub>O was sealed in a 25 mL Teflon-lined stainless steel container and heated at 130  $^\circ C$  for 3 days. After the mixture was cooled to room temperature at a rate of 5  $^\circ C h^{-1}$ , colorless block crystals of **5** were obtained with a yield of 65 % (based on Cd). Anal. calcd for  $C_{24}H_{21}N_4O_4Cd$  (%): C, 53.20; H, 3.91; N, 10.34. Found: C, 53.55; H, 3.64; N, 10.61. IR (KBr,  $cm^{-1}$ ): 3422(w), 3126(w), 1565(m), 1484(m), 1378(s), 1290(m), 1017(m), 873(s), 745(s), 576(m), 511(m).

**Synthesis of  $\{[Cd(pbmb)(sdba)] \cdot 2H_2O\}_n$  (**6**).** Complex **6** was prepared by the similar synthetic procedure of **5** with a yield of 89 % (based on Cd). Anal. calcd for  $C_{33}H_{32}N_4O_8SCd$  (%): C, 52.35; H, 4.26; N, 7.40; S 4.33. Found: C, 52.77; H, 4.13; N, 7.80; S, 3.96. IR (KBr,  $cm^{-1}$ ): 3648(w), 3609(w), 3458(w), 3104(w), 3061(w), 2938(w), 1595(m), 1552(m), 1515(m), 1455(m), 1405(s), 1323(m), 1293(m), 1236(m), 1161(m), 1099(m), 1015(m), 934(m), 857(s), 746(s), 698(m), 621(m),

579(m), 462(m).

**Crystal Data Collection and Refinement.** The data for complexes **1–6** were collected on a Rigaku Saturn 724 CCD diffractometer (Mo- $K\alpha$ ,  $\lambda = 0.71073$  Å) at temperature of  $20 \pm 1$  °C. Absorption corrections were applied by using multi-scan program. The data were corrected for Lorentz and polarization effects. The structures were solved by direct methods and refined with a full-matrix least-squares technique based on  $F^2$  with the SHELXL-97 crystallographic software package.<sup>17</sup> Hydrogen atoms were placed at calculated positions and refined as riding atoms with isotropic displacement parameters. In the structures of compounds **2**, **4** and **6**, some oxygen atoms without hydrogen atom were modelled as solvent water or the hydroxo ligand. The water molecules in **3** were removed by the SQUEEZE routine in PLATON. The numbers of solvent molecules were obtained by element analyses and TGA. Crystallographic crystal data and structure processing parameters for **1–6** are summarized in Table S1 (Supporting Information). Selected bond lengths and bond angles of **1–6** are listed in Table S2. Crystallographic data for **1–6** have been deposited at the Cambridge Crystallographic Data Centre with CCDC reference numbers 979662–979667.

**Optical band gap and photocatalytic measurement.** The diffuse-reflectance UV–vis spectra of CPs **1–6** in solid states were obtained on a Cary 500 spectrophotometer equipped with a 110 nm diameter integrating sphere to calculate the optical band gaps ( $E_g$ ) by the Kubelka-Munk function ( $F(R) = (1-R)^2/2R$ , where  $R$  was the reflectance of an infinitely thick layer at a given wavelength. 30 mg CPs and 5  $\mu$ L of 30 %  $H_2O_2$  were added into 80 mL of methylene blue (MB) aqueous solutions ( $5 \times 10^{-5}$  mol/L), respectively, then magnetically stirred in the dark for about 60 minutes to guarantee the establishment of an sorption/desorption equilibrium. The solution was then exposed to irradiation under a high-pressure mercury lamp (500 w). At ca. 20 min intervals, 6 mL supernatant were taken out from the vessel, and subsequently analyzed by UV-visible spectrometer. The typical absorption band of MB ( $\lambda_{max} = 664$  nm) was selected for monitoring the photocatalytic degradation process. All the UV–vis absorption spectra in water were collected on a TU-1901 double-beam UV–Vis Spectrophotometer.

## Results and discussion

### Crystal Structure of $[Cd(pbmb)(p-bdc)]_n$ (**1**)

The X-ray crystallographic analysis reveals that the complex **1** crystallizes in the monoclinic space group  $P2_1/c$  and features a three-dimensional (3D) metal-organic framework. In the asymmetric unit of **1**, there exists one crystallographically independent Cd(II) ion, one pbmb ligand and one  $p-bdc^{2-}$  anion. As shown in Figure S1a, Cd(II) sits in a distorted octahedral geometry defined by three oxygen atoms (O1, O3A and O4A) from two different  $p-bdc^{2-}$  anions and one nitrogen atom (N1) from one pbmb ligand composing the equatorial plane; one oxygen atom (O2) and one nitrogen atom (N4B) from another pbmb ligand at the axial sites. The Cd–O/N bond lengths are 2.278(3)–2.459(3) Å and 2.287(3)–2.292(3) Å, respectively, which are all in conformity with the corresponding bond lengths in reported works.<sup>18</sup> The  $p-bdc^{2-}$  anions, as auxiliary ligands, with  $\mu_1-\eta^1:\eta^1$ ,  $\mu_1-\eta^1:\eta^1$  coordination mode, connect adjacent Cd(II)

atoms to generate an infinite chain (Figure 1a). Moreover, the flexible pbmb ligands adopt asymmetrical *trans*-conformation and act as bidentate mode to link adjacent Cd(II) ions alternately to generate a zigzag chain. The interlaced connection of these chains further gives rise to a complicated 3D framework (Figure 1b). Furthermore, topological analysis is performed to get better insight into the nature of complex **1**. Considering the Cd atom as a four-connected node and the  $p-bdc^{2-}$  ligands and pbmb ligands as linkers, the whole structure of **1** can be simplified to a 3D framework with topological notation of  $6^6$  (Figure S1b).

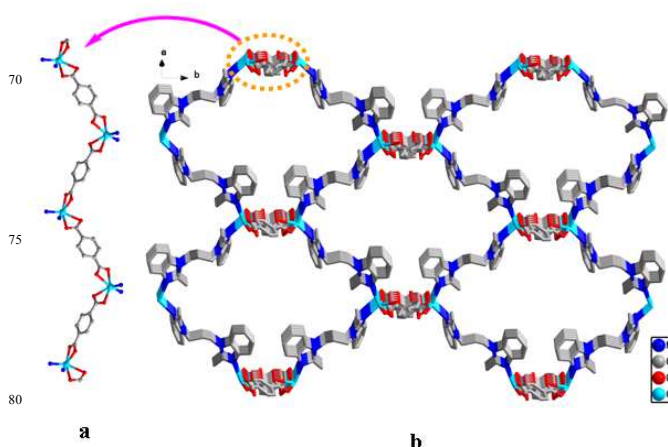


**Figure 1.** (a) the infinite chain formed by Cd(II)/ $p-bdc^{2-}$ ; (b) Perspective view of the 3D coordination framework constructed by Cd(II)/ $p-bdc^{2-}$  and Cd(II)/pbmb chains.

### Crystal Structure of $\{[Zn_3(pbmb)_2(1,3,5-btc)] \cdot 6H_2O\}_n$ (**2**)

Complex **2** shows a triclinic space group  $P\bar{1}$ , which is also an infinite 3D coordination framework. Its asymmetric unit contains three crystallographically independent Zn(II) ions, two pbmb ligands, two 1,3,5- $btc^{3-}$  anions, and six guest water molecules. In Figure S2a, the Zn1 and Zn2 ions exhibit similar coordination environments, which are four-coordinated by three oxygen atoms from three different 1,3,5- $btc^{3-}$  anions, and one nitrogen atom from one pbmb ligand, representing a slightly distorted tetrahedron geometry. The Zn1 and Zn2 ions are bridged together by a pair of carboxylate groups from two 1,3,5- $btc^{3-}$  ions into a binuclear unit  $[Zn_2(CO_2)_2]$ , with an average Zn–O/nonbonding Zn...Zn distance<sup>19</sup> of 1.962/3.847 Å, respectively. The Zn3 ion also displays a distorted tetrahedron geometry, with two oxygen atoms (Zn3–O1 = 1.929(4) Å, Zn3–O7D = 1.940(4) Å) provided by two different 1,3,5- $btc^{3-}$  anions and two nitrogen atoms (Zn3–N1C = 1.997(4) Å, Zn3–N8E = 2.008(4) Å) provided by two different pbmb ligands. All of the Zn–O/Zn–N distance parameters fall into the normal range.<sup>20</sup> As illustrated in Figure 2a, the 1,3,5- $btc^{3-}$  anions, as auxiliary ligands, were completely deprotonated and three carboxylate groups participate in coordination with  $\mu_1-\eta^0:\eta^1$ ,  $\mu_1-\eta^0:\eta^1$ , and  $\mu_2-\eta^1:\eta^1$  mode connecting Zn ions to form a 2D layer. Additionally, the extension of the structure into a 3D network is also completed by connecting two adjacent 2D layers through pbmb ligands in asymmetrical *trans*-conformation (Figure 2b). From the topological point of view, the  $[Zn_2(CO_2)_2]$  dimeric unit is taken as a 6-connected node, the Zn3 atom is considered as a 4-connected node and the 1,3,5- $btc^{3-}$  anion can be viewed as a 3-connected node. Accordingly, the 3D

complex framework of **2** can be described as a rare (3, 4, 6)-connected topology with the topological notation of  $(6^5.7)(4.6^2)_2(4^2.6^6.8^5.10^2)$  (Figure 2c).

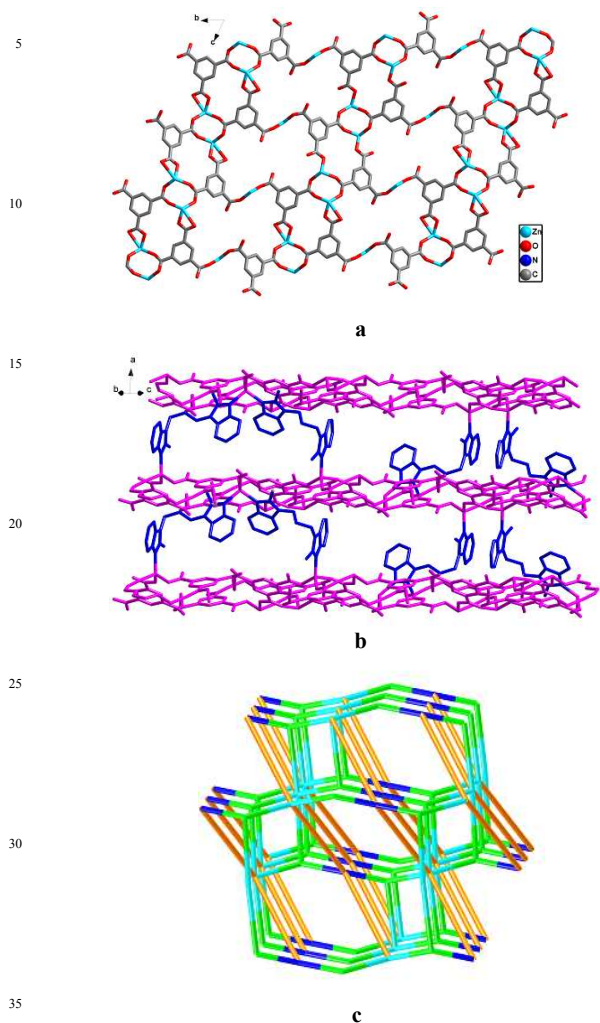


**Figure 2.** (a) 2D layer of **2** formed by Zn/btc<sup>3-</sup>; (b) Perspective view of the 3D coordination framework constructed by Zn(II)/1,3,5-btc<sup>3-</sup> layers and pbmb ligands; (c) Schematic illustrating the (3, 4, 6)-connected topology with the topological notation of  $(6^5.7)(4.6^2)_2(4^2.6^6.8^5.10^2)$ .

### Crystal Structure of $\{[\text{Cd}_3(\text{pbmb})_3(1,3,5\text{-btc})_2(\text{H}_2\text{O})]\cdot 3\text{H}_2\text{O}\}_n$ (**3**)

In consideration of the importance of different coordination modes in constructing diverse structures, we replaced metal salts and got a significantly different 3D framework comparing with **2**. The asymmetric unit of **3** contains three crystallographically independent Cd(II) ions, three pbmb ligands, two 1,3,5-btc<sup>3-</sup> anions, one coordinated water molecule and three disordered solvent water molecules modelled by SQUEEZE. Cd1 ion possesses six-coordinated octahedral geometry (Figure S3a), which is ligated by four oxygen atoms from two different 1,3,5-btc<sup>3-</sup> ions and two nitrogen atoms from two pbmb ligands [Cd1–O = 2.297(4)–2.424(5) Å, Cd1–N = 2.265(5), 2.276(5) Å]. Cd2 ion is five-coordinated by three oxygen atoms from two different 1,3,5-btc<sup>3-</sup> ions [Cd2–O = 2.200(5)–2.371(5) Å] and two nitrogen atoms from two pbmb ligands [Cd2–N = 2.246(5),

2.318(5) Å] showing a distorted square-pyramidal arrangement. In this square-pyramid, O5A, O12, O13 and N4B lie in the basal plane and N12C inhabits the apex. Cd3 possesses an distorted octahedral geometry formed by four oxygen atoms from two different 1,3,5-btc<sup>3-</sup> ions, one oxygen atom from one coordinated water molecule and one pbmb ligand [Cd3–O = 2.199(5)–2.619(7) Å, Cd3–N = 2.294(5) Å]. Notably, the 1,3,5-btc<sup>3-</sup> anions bridge the Cd(II) ions by adopting  $\mu_1\text{-}\eta^1\text{:}\eta^1$ ,  $\mu_1\text{-}\eta^1\text{:}\eta^1$ ,  $\mu_1\text{-}\eta^1\text{:}\eta^1$  and  $\mu_1\text{-}\eta^0\text{:}\eta^1$ ,  $\mu_1\text{-}\eta^1\text{:}\eta^1$ ,  $\mu_1\text{-}\eta^1\text{:}\eta^1$  coordination fashions to form a double chain. The pbmb ligands, which exhibits asymmetrical *cis*-conformation, connect adjacent Cd(II) ions derived from two different double chains to form another zigzag chain as shown in Figure 3a. The alternate arrangement of the Cd(II)-pbmb and Cd(II)-1,3,5-btc<sup>3-</sup> chains constructs the 3D framework of **3** by sharing Cd(II) ions (Figure 3b). With further topological analysis, the Cd1 and Cd2 ions can be defined as 4-connected nodes, the Cd3 ions can be simplified as 2-connected nodes and the btc<sup>3-</sup> anions can be considered as 3-connected nodes. Therefore, the 3D structure can be described as a (2, 3, 4)-connected topology with point symbol of  $(6^5.8)_2(6^3)_2$  (Figure S3b).

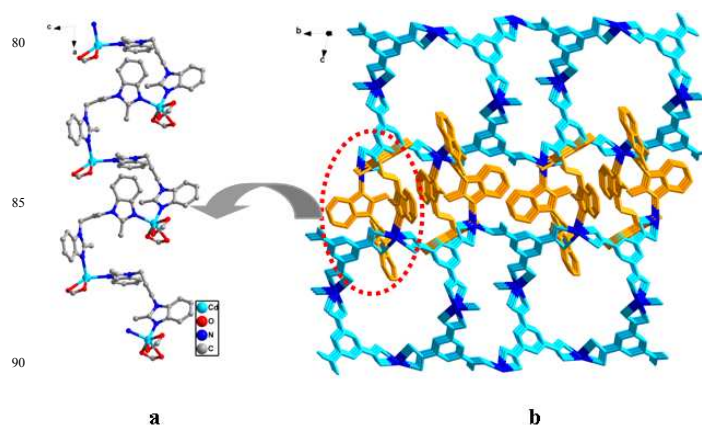


**Figure 3.** (a) The zigzag chain of **3** formed by Cd/pbmb ligands; (b) Perspective view of the 3D coordination framework constructed by Cd(II)/1,3,5-btc<sup>3-</sup> and Cd(II)/pbmb ligands chains.

### Crystal Structure of $\{[\text{Zn}_2(\text{pbmb})(1,2,3\text{-btc})(\mu_2\text{-OH})\cdot \text{H}_2\text{O}]\}_n$ (**4**)

Analysis of **4** exhibits that its asymmetric unit contains two Zn(II) ions, one pbmb ligands, one 1,2,3-btc<sup>3-</sup> anions, one  $\mu_2$ -OH and one guest water molecule. The two Zn(II) ions have the same coordination environment in an tetrahedral coordination sphere, which is completed by three oxygen atoms from two 1,2,3-btc<sup>3-</sup> anions and one water molecule and one nitrogen atom from one pbmb ligand (Figure 4a). One carboxylate group from the 1,2,3-btc<sup>3-</sup> ion and one hydroxyl ion engaged the Zn1 and Zn2 ions into the binuclear cluster  $[\text{Zn}_2\text{C}_2\text{O}_3]$ , with the Zn $\cdots$ Zn distance<sup>19</sup> of 3.2441 Å. The Zn–O/N bond lengths are 1.942(6)–2.004(6)/2.008(6)–2.010(7) Å, respectively, which are all similar to those found in other Zn(II) complexes.<sup>20</sup> The three carboxyl groups of the 1,2,3-btc<sup>3-</sup> ion are completely deprotonated and adopt the coordination modes of  $\mu_2\text{-}\eta^1\text{:}\eta^1$ ,  $\mu_1\text{-}\eta^0\text{:}\eta^1$  and  $\mu_1\text{-}\eta^0\text{:}\eta^1$  to connect Zn(II) atoms to form a 2D layer containing two kinds of rings (Figure S4a). One is a little ring constructed by the bridge of two 1,2,3-btc<sup>3-</sup> ions between two

binuclear Zn(II) clusters, another is a elliptical ring constructed by the connection of four 1,2,3-btc<sup>3-</sup> ions among four binuclear Zn(II) clusters. Herein, two pbmb ligands adopt a bidentate fashion to join Zn(II) ions in the elliptical ring, which may further stabilize the 2D layers (Figure 4b). From a topological perspective of Figure S4b, the binuclear Zn(II) clusters and 1,2,3-btc<sup>3-</sup> ions act as 5-connected and 3-connected nodes, respectively, giving rise to a (3, 5)-connected 2D network with the Schläfli symbol of (3.6<sup>2</sup>)(3.6.7)(3.4.5)(3<sup>2</sup>.4.5.6<sup>2</sup>.7<sup>4</sup>).

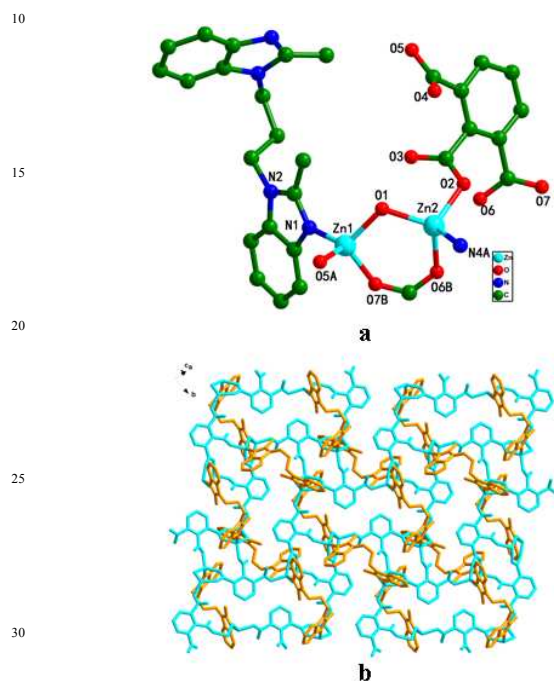


**Figure 4.** (a) Coordination environment of Zn(II) ion in **4**. Hydrogen atoms and the 35 free water molecule are omitted for clarity. Symmetry operator: A = 0.5-x, -0.5+y, 1.5-z; B = 1-x, -y, 2-z; (b) Perspective view of 2D layer connected by Zn(II)/1,2,3-btc<sup>3-</sup> and pbmb ligands.

#### Crystal Structure of [Cd(pbmb)(1,2,4,5-btec)<sub>0.5</sub>]<sub>n</sub> (**5**)

Complex **5** crystallizes in the triclinic space group P1. One Cd(II) ion, one pbmb ligand and half a deprotonated 1,2,4,5-btec<sup>4-</sup> anion are in the asymmetric unit of **5**. As shown in Figure S5a, the Cd(II) ion adopts a distorted octahedral geometry which is completed by three oxygen atoms (O1, O2, O4B) from two 1,2,4,5-btec<sup>4-</sup> anion and one nitrogen atom (N4C) from one pbmb ligand composing the equatorial plane, and one oxygen atom (O3B) from one of the 1,2,4,5-btec<sup>4-</sup> anion and one nitrogen atom (N1) from another pbmb ligand at the apical positions. The bond lengths of Cd-O and Cd-N are similar to those in other cadmium coordinated complexes.<sup>18</sup> All of the carboxylate groups of btec<sup>4-</sup> anion adopt  $\mu_1-\eta^1:\eta^1$  coordination mode and connect Cd(II) ions to form a 1D infinite chain. And then, the chains are engaged by pbmb ligands to give rise to an interesting 2D layer, where two pbmb ligands connect two Cd(II) ions from adjacent 1D chains into the M<sub>2</sub>L<sub>2</sub>-type loop (Figure 5a). From topological point, the Cd(II) ions are viewed as 3-connected nodes, btec<sup>4-</sup> ions are viewed as 4-connected nodes and pbmb ligands are simplified as linkers. The resulting structure can be described as a 2D network

with point (Schläfli) symbol of (4.6<sup>2</sup>)(4<sup>2</sup>.6<sup>2</sup>.8<sup>2</sup>) (Figure S5b). In addition, as shown in Figure 5b, there exist weak  $\pi\cdots\pi$  stacking interactions (inidazole to inidazole distance of 3.526(3) Å, in Figure 5c) between the pbmb ligands in the neighboring layers contributing to the formation of a 3D supramolecular framework.

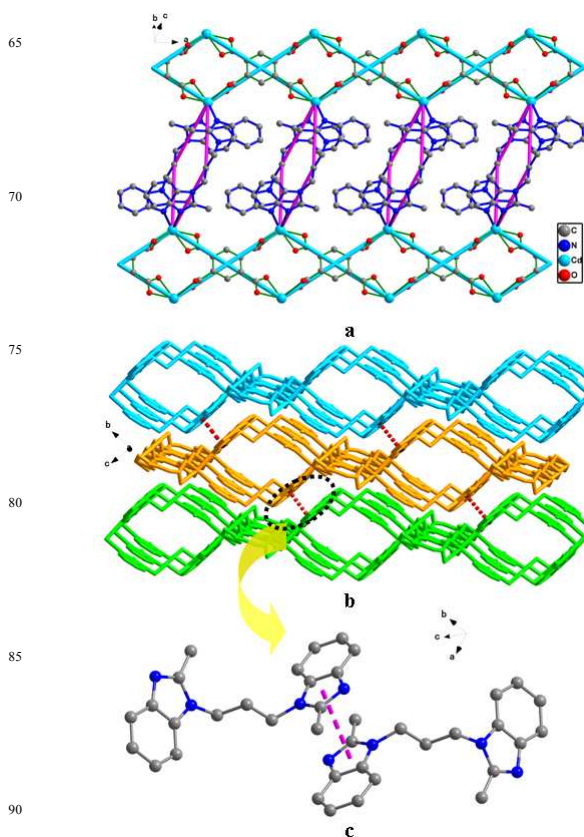


**Figure 5.** (a) 2D layer of **5** formed by Zn/btec<sup>4-</sup> and pbmb ligands; (b) Perspective view of the 3D supramolecular framework constructed by the  $\pi\cdots\pi$  stacking; (c) The  $\pi\cdots\pi$  interaction between inidazoles.

#### Crystal Structure of {[Cd(pbmb)(sdba)·2H<sub>2</sub>O]<sub>n</sub> (**6**)

In the monoclinic space group P2<sub>1</sub>/c, the asymmetric unit of **6** contains one Cd(II) ion, one pbmb ligand, one sdba<sup>2-</sup> anion, and two guest water molecules. As depicted in Figure S6a, the Cd(II) ion is octahedrally coordinated by four oxygen atoms from two chelating bidentate carboxylate group [Cd-O = 2.268(3) – 2.505(3) Å] and two nitrogen atoms from two pbmb ligands [Cd-N = 2.268(3) – 2.291(3) Å], which are within the normal distances of those observed in Cd(II)-contained complexes.<sup>18</sup> Adjacent Cd(II) ions are linked by  $\mu_2$ -bridging sdba<sup>2-</sup> anions to yield left- and right-handed helical chains. Both of the helical chains are 18.8 Å, which correspond to the length of *b* axis. Two pbmb ligands connect two Cd(II) ions from the left and right-handed helical chains, respectively, into the M<sub>2</sub>L<sub>2</sub>-type loop with the Cd $\cdots$ Cd distance<sup>21</sup> of 10.4375 Å (Figure 6a). Therefore, the 1D helical chains are further connected by the M<sub>2</sub>L<sub>2</sub>-type loop to form a 2D network (Figure 6b). From topological point, the Cd(II) ions are viewed as 3-connected nodes and the sdba<sup>2-</sup> ions and pbmb ligands are simplified as linkers, the resulting structure can be described as a 2D network with point (Schläfli) symbol of 6<sup>3</sup> (Figure S6b).

### Influence of different auxiliary aromatic polycarboxylates on the structures of complex 1–6

As we know, aromatic polycarboxylates have a great influence on the constructing of the multidimensional coordination polymers, due to its diversiform coordination modes, the number of carboxylate groups, different carboxylate position and distinct flexibility of organic skeletons.<sup>22</sup> According to the above-mentioned structural descriptions, the impact of different auxiliary aromatic polycarboxylates on the structures of multidimensional CPs is undoubtedly remarkable.

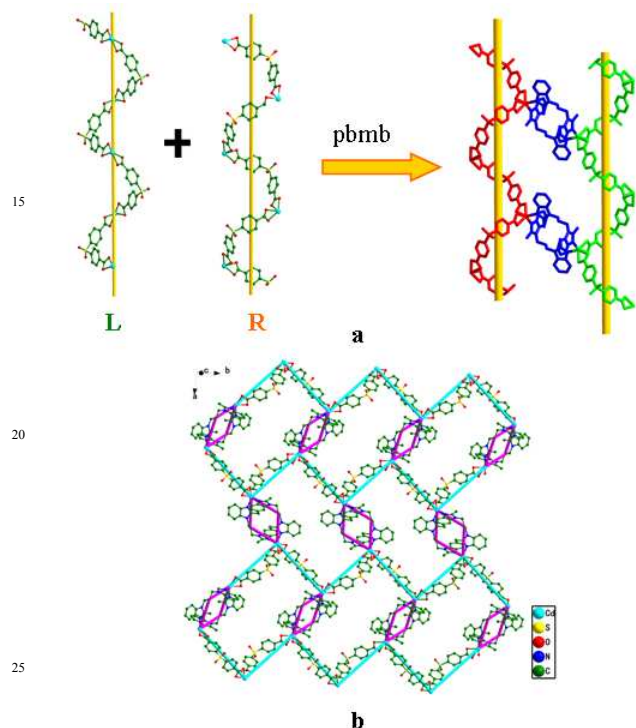


**Figure 6.** (a) Perspective view of the left- and right-handed helical chains and  $M_2L_2$ -type loop; (b) 2D layer of **6** formed by  $Zn/sdba^{2-}$  and pbmb ligands.

In complex **1** and **3**,  $p\text{-bdc}^{2-}$  and  $1,3,5\text{-btc}^{3-}$  anions connect the adjacent Cd(II) atoms to generate an infinite chain and a double chain, respectively. And then, the alternate arrangement of Cd- $p\text{-bdc}^{2-}/1,3,5\text{-btc}^{3-}$  chains and Cd-pbmb chains builds two 3D frameworks, **1** and **3**. Interestingly, complex **2** demonstrates that the  $1,3,5\text{-btc}^{3-}$  anions participate in  $\mu_1\text{-}\eta^0\text{:}\eta^1$ ,  $\mu_1\text{-}\eta^0\text{:}\eta^1$ , and  $\mu_2\text{-}\eta^1\text{:}\eta^1$  coordination mode connecting Zn atoms to form a 2D layer. The pbmb ligands bridge 2D layers to generate a rarely (3, 4, 6)-connected topology with the topological notation of  $(6^5.7)(4.6^2)_2(4^2.6^6.8^5.10^2)$ . In case **4**, the  $1,2,3\text{-btc}^{3-}$  anions participate in the same coordination mode connecting Zn atoms to form a different 2D layer containing two kinds of rings. Moreover, pbmb ligands join Zn(II) ions in the elliptical ring, which may further stabilize the 2D layers. Btec<sup>4-</sup> anions connect Cd(II) ions to form a 1D infinite chain in complex **5**, which are engaged by  $M_2L_2$ -type loops to obtain an interesting (3,4)-connected 2D layer. In addition, weak  $\pi\cdots\pi$  stacking interactions contribute to the formation of a 3D supramolecular framework. However, in complex **6**, Cd(II) ions are linked by  $\mu_2$ -bridging

$sdba^{2-}$  anions to yield left and right-handed helical chains. Connecting  $M_2L_2$ -type loops, the helical chains are extended into a 3-connected 2D network. Most strikingly, in complex **2** and **3**, the  $1,3,5\text{-btc}^{3-}$  anions link metal ions by different coordination modes to construct miraculous structures, which demonstrates that diversiform coordination modes indeed have an important influence on the constructing of the multidimensional CPs.

### Thermal stability and PXRD of complexes 1–6

For coordination polymers as potential function materials, the detection of their thermal stability is particularly necessary. Herein, thermogravimetric analyses (TGA) of complexes **1–6** were performed as shown in Figure S7. For anhydrous complex **1** or **5**, the decomposition of the organic ligand occurs in the temperature ranging from 365 °C or 420 °C, respectively. The remaining weight loss is in accordance with the formation of CdO (**1**: obsd, 22.17%, calcd 22.10 %; **5**: obsd 23.56 %, calcd 23.70 %). In complex **2**, TGA curve exhibits that a weight loss of 7.97 % from 80 to 280 °C corresponds to the release of six lattice water molecules (calcd, 8.14 %) and the organic components decomposed from 433 °C. The remaining residue is 18.23% corresponding to the formation of ZnO (calcd 18.40 %). The first weight loss of complex **3** takes place at 76–280 °C and corresponds to the loss of two guest H<sub>2</sub>O molecules and one coordinated water molecule (obsd, 3.98 %; calcd, 4.15 %). The crystal structure collapses from 360 °C and the remaining weight corresponds to the formation of CdO (obsd, 22.45 %; calcd 22.18 %). In the first step in the range of 69.6–280 °C, complex **4** lose 2.57 % weight corresponds to the removal of one lattice water molecule (calcd, 2.66 %). Decomposition of the organic ligands began above 380 °C. The residue corresponds to the formation of ZnO (obsd, 24.40 %; calcd, 24.03 %). For complex **6**, the weight loss of 4.67 % in the first step (78–265 °C) corresponds to the removal of two lattice water molecules (calcd 4.75 %) and the decomposition of the organic ligands began above 343 °C. The remaining weight loss is in accordance with the formation of CdO (obsd, 17.14 %; calcd 16.96 %).

Furthermore, the PXRD patterns for complexes **1–6** are shown in the Figure S8. The diffraction peaks of experimental patterns match well with simulated data, indicating that the synthesized bulk materials are consistent with the measured single crystals.

### Optical Band Gap

The diffuse-reflectance UV-vis spectra of pbmb ligand, five aromatic polycarboxylates and the six complexes were recorded in solid state at room temperature (Figure S9). The pbmb ligand exhibits intense absorption bands of the typical  $\pi\rightarrow\pi^*$  transitions at 208 nm and 256nm. Moreover, the UV-vis spectra of five aromatic polycarboxylates show different absorption bands with maxima at 243nm and 317nm for  $p\text{-H}_2\text{bdc}$ , 243nm and 294nm for  $1,3,5\text{-H}_3\text{btc}$ , 241nm and 296nm for  $1,2,3\text{-H}_3\text{btc}$ , 239nm and 310nm for  $1,2,4,5\text{-H}_4\text{btec}$  and 253nm and 302nm for  $\text{H}_2\text{sdba}$ , which are ascribed to the  $\pi\rightarrow\pi^*$  transitions. Remarkably, all of the lowest energy absorption bands in the aromatic carboxylate ligands are lower than that of pbmb ligand in the energy level, which indicates that they might be more influenced than the lowest energy absorption band of pbmb ligand by the coordination with the transition metal ion.

In comparison with the corresponding aromatic carboxylate ligands *p*-H<sub>2</sub>bdc ( $\lambda_{\max} = 317 \text{ nm}$ ,  $31545 \text{ cm}^{-1}$ ) and 1,3,5-H<sub>3</sub>btc ( $\lambda_{\max} = 294 \text{ nm}$ ,  $34015 \text{ cm}^{-1}$ ), complexes **1** and **3** exhibit that the lowest energy absorption bands are apparently blue-shifted ( $\lambda_{\max} = 276 \text{ nm}$ ,  $36230 \text{ cm}^{-1}$ ;  $\lambda_{\max} = 273 \text{ nm}$ ,  $36630 \text{ cm}^{-1}$ , respectively), which may be assigned to the coordination of the carboxylate group to the Cd(II) ion increasing the energy gap of the intraligand (IL,  $\pi \rightarrow \pi^*$ ) transition in nature. In contrast, the lowest energy absorption band of complex **2** slightly shifts according to that of the 1,3,5-H<sub>3</sub>btc, probably resulting from the coordination mode of Zn(II) metal ion and the aromatic carboxylate group. Notably, to compare those of 1,2,3-H<sub>3</sub>btc, 1,2,4,5-H<sub>4</sub>btec and H<sub>2</sub>sdba, the absorption spectra of complexes **4**, **5** and **6** are slightly red-shifted, respectively. For example, complex **5** displayed about 5 nm red-shift, which may be attributed to the decreased the energy gap of the IL ( $\pi \rightarrow \pi^*$ ) transition by the intervention of the metal center ion.

In the reported coordination polymer examples,<sup>12a, 14, 23</sup> the optical band gap ( $E_g$ ) was one key factor for the efficiency of the photocatalytic decomposition of the organic dyes, which were distinctly connected with the constructions of the CPs. Herein, the reflectance spectra are converted into absorption-like spectra by using the Kubelka-Munk equation to calculate the band gap  $E_g$ . The  $F$  versus  $E$  plots are shown in Figure S10, and the  $E_g$  values assessed from the steep absorption edge for complexes **1–6** are 3.60, 3.62, 3.72, 3.04, 3.40 and 3.08 eV, respectively. The reflectance spectra reveal that the presence of an optical band gap and the nature of semiconductivity for complexes **1–6**, which indicates that these complexes are potential semiconductive materials. Moreover, complex **4** might show the best behaviors in photocatalytic degradation of the dye contaminant, because of the smallest band gaps, and the efficiency of **6** would be close to that of **4**.

### Photocatalysis property

To study the photocatalytic behavior of complexes **1–6** in detail, methylene blue (MB) was selected as a model of dye contaminant, to evaluate the efficiency of photocatalysts in purifying wastewater. The solution was exposed to the irradiation from a 500 W high pressure mercury vapor lamp at a distance of 5 cm between the liquid surface and the lamp. The photodegradation process of MB without any catalyst had also been studied for the control experiment. The change of typical absorption band of MB is illustrated under the different reaction time in Figure S11. In addition, the concentrations of MB ( $C$ ) versus reaction time ( $t$ ) of complexes **1–6** are plotted in Figure 7 (wherein,  $C_0$  is the initial concentration of the MB and  $C_t$  is the concentration of the dye on any given time).

As show in Figure S11, all the synthetic CPs perform the obvious photocatalytic behavior to decompose the MB in water, especially complexes **1**, **4** and **6**. Furthermore, according to Figure 7, the total photocatalytic efficiency of control experiment is 20 %. In comparison with that, the systems with different photocatalysts **1–6**, indicate much better consequences for the MB cancellation (**1**: 74 %, **2**: 41 %, **3**: 37 %, **4**: 76%, **5**: 46%, **6**: 75%, respectively). The results displayed that complex **1**, **4** and **6** are more efficient than complex **2**, **3** and **5** for the decomposition

of MB under the light irradiation (**3**<**2**<**5**<**1**≈**6**≈**4**), which is mostly consistent with the reverse order of the band gap trend of complexes **1–6** (**3**>**2**≈**1**>**5**>**6**≈**4**). The photocatalytic research result indicates that complexes **1**, **4**, **6** may be good heterogeneous catalysts for the light-driven degradation of MB in water. Curiously, to deliberate to relatively large band gap of 3.60 eV, complex **1** exhibits the high photocatalytic efficiency, which is close to the best examples **4** and **6**. The high photocatalytic efficiency of complex **1** may be due to the distinct 3D framework constructed by pbmb ligands and *p*-bdc<sup>2-</sup> ions to accelerate the electron ( $e^-$ ) and hole ( $h^+$ ) transfer process or gear up the sorption of O<sub>2</sub>/OH<sup>-</sup> on the CPs. The specific reasons about the distinct structure need be further investigated.

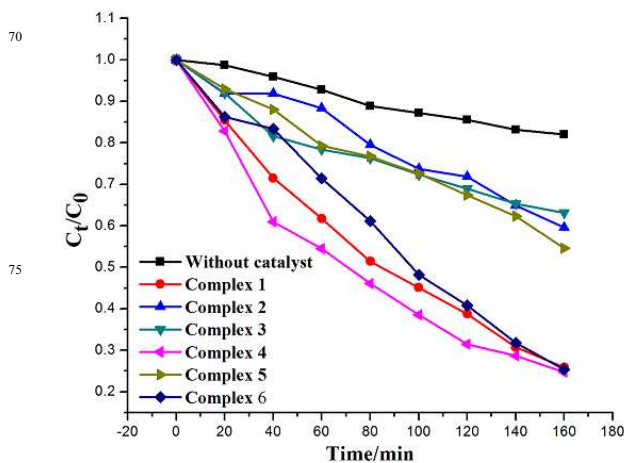


**Figure 7.** Photocatalytic decomposition of MB solution under UV light irradiation with the use of complexes **1–6** and the control experiment without any catalyst ( $C_0$  is the initial concentration of the MB and  $C_t$  is the concentration of the dye on any given time).

### Conclusions

In summary, we have successfully synthesized six interesting coordination polymers, tuned by different aromatic polycarboxylates, displaying diverse structural features and charming topologies. Photocatalytic experiment results indicate that complexes **1–6** are photocatalytically active for the degradation of MB under high-pressure mercury lamp irradiation, which may be good candidates for the photocatalytic degradation of other organic dyes.

### Acknowledgment.

This work was financially supported by the National Natural Science Foundation (Nos. 21371155; 21301157) and Research Found for the Doctoral Program of Higher Education of China (20124101110002).

### References

- (1) (a) H. Furukawa, N. Ko, Y. B. Go, N. Aratani, S.B. Choi, E. Choi, A. O. Yazaydin, R. Q. Snurr, M. O'Keeffe, J. Kim and O. M. Yaghi, *Science*, 2010, **329**, 424. (b) M. L. Foo, S. Horike, Y. Inubushi and S. Kitagawa, *Angew. Chem., Int. Ed.*, 2012, **51**, 6107. (c) Y. Y. Liu, S. Couck, M. Vandichel, M. Grzywa, K. Leus, S. Biswas, D. Volkmer, J. Gascon, F. Kapteijn, J. F. M. Denayer, M. Waroquier,

- V. V. Speybroeck and P. V. D. Voort, *Inorg. Chem.*, 2013, **52**, 113. (d) J. H. Luo, H. W. Xu, Y. Liu, Y. S. Zhao, L. L. Daemen, C. Brown, T. V. Timofeeva, S. Q. Ma and H. C. Zhou, *J. Am. Chem. Soc.*, 2008, **130**, 9626. (e) L. Q. Ma, A. Jin, Z. G. Xie, W. B. Lin, *Angew. Chem., Int. Ed.*, 2009, **48**, 9905.
- (2) (a) M. Y. Yoon, R. Sriramalaji, K. Kim, *Chem. Rev.*, 2012, **112**, 1196. (b) D.W. Feng, Z. Y. Gu, J. R. Li, H. L. Jiang, Z. W. Wei and H. C. Zhou, *Angew. Chem., Int. Ed.*, 2012, **51**, 10307. (c) J. M. Roberts, B. M. Fini, A. A. Sarjeant, O. K. Farha, J. T. Hupp and K. A. Scheidt, *J. Am. Chem. Soc.*, 2012, **134**, 3334. (d) Z. L. Liao, G. D. Li, M. H. Bi, J. S. Chen, *Inorg. Chem.*, 2008, **47**, 4844. (e) J. M. Zhang, A. V. Biradar, S. Pramanik, T. J. Emge, T. Asefa and J. Li, *Chem. Commun.*, 2012, **48**, 6541. (f) L. Q. Ma, C. Abney and W. B. Lin, *Chem. Soc. Rev.*, 2009, **38**, 1248.
- (3) (a) Z. M. Wang, Y. J. Zhang, T. Liu, M. Kurmoo and S. Gao, *Adv. Funct. Mater.*, 2007, **17**, 1523. (b) Z. R. Pan, H. G. Zheng, T. W. Wang, Y. Song, Y. Z. Li, Z. J. Guo, S. R. Batten, *Inorg. Chem.*, 2008, **47**, 9528. (c) J. P. Zhao, Q. Yang, Z. Y. Liu, R. Zhao, B. W. Hu, M. Du, Z. Chang and X. H. Bu, *Chem. Commun.*, 2012, **48**, 6568. (d) N. Yanai, W. Kaneko, K. Yoneda, M. Ohba and S. Kitagawa, *J. Am. Chem. Soc.*, 2007, **129**, 3496. (e) P. Lama, J. Mrozinski and P. K. Bharadwaj, *Cryst. Growth Des.*, 2012, **12**, 3158. (f) S. H. Cho, B. Ma, S. T. Nguyen, J. T. Hupp, T. E. Albrecht-Schmitt, *Chem. Commun.*, 2006, **24**, 2563.
- (4) (a) Alberola, A., Coronado, E., Galán-Mascarós, J. R., Giménez-Saiz, C., Gómez-García, *J. Am. Chem. Soc.*, 2003, **125**, 10774. (b) H. Okawa, M. Sadakiyo, T. Yamada, M. Maesato, M. Ohba, and H. Kitagawa, *J. Am. Chem. Soc.*, 2013, **135**, 2256. (c) U. Subbarao and S. C. Peter, *Cryst. Growth Des.*, 2013, **13**, 953. (d) E. Coronado, J. R. Galán-Mascarós, C. J. Gómez-García, V. Laukhln, *Nature*, 2000, **408**, 447.
- (5) (a) F. Nouar, J. Eckert, J. F. Eubank, P. Forster and M. Eddaoudi, *J. Am. Chem. Soc.*, 2009, **131**, 2864. (b) X. L. Zhao, X. Y. Wang, S. N. Wang, J. M. Dou, P. P. Cui, Z. Chen, D. Sun, X. P. Wang and D. F. Sun, *Cryst. Growth Des.*, 2012, **12**, 2736. (c) J. R. Choi, T. Tachikawa, M. Fujitsuka, T. Majima, *Langmuir*, 2010, **26**, 10437. (d) C. A. Bauer, T. V. Timofeeva, T. B. Settersten, B. D. Patterson, V. H. Liu, B. A. Simmons, M. D. Allendorf, *J. Am. Chem. Soc.*, 2007, **129**, 7136. (e) K. A. White, D. A. Chengelis, K. A. Gogick, J. Stehman, N. L. Rosi and S. Petoud, *J. Am. Chem. Soc.*, 2009, **131**, 18069. (f) J. R. Li, Y. Tao, Q. Yu, X. H. Bu, *Chem. Commun.*, 2007, 1527. (g) B. Dey, R. Saha, P. Mukherjee, *Chem. Commun.*, 2013, **49**, 7064.
- (6) (a) P. V. Dau, K. K. Tanabe and S. M. Cohen, *Chem. Commun.*, 2012, **48**, 9370. (b) Q. Liu, L. N. Jin and W. Y. Sun, *Chem. Commun.*, 2012, **48**, 8814. (c) J. Yang, J. F. Ma, S. R. Batten and Z. M. Su, *Chem. Commun.*, 2008, **19**, 2233. (d) V. A. Blatov, M. O'Keeffe and D. M. Proserpio, *CrystEngComm*, 2010, **12**, 44. (e) S. C. Chen, R. R. Qin, Z. H. Zhang, J. Qin, H. B. Gao, F. A. Sun, M. Y. He and Q. Chen, *Inorg. Chim. Acta.*, 2012, **390**, 61. (f) M. Wriedt, A. A. Yakovenko, G. J. Halder, A. V. Prosvirin, K. R. Dunbar and H. C. Zhou, *J. Am. Chem. Soc.*, 2013, **135**, 4040. (g) F. F. Pan, R. Wang, U. Englert, *Inorg. Chem.*, 2012, **51**, 769.
- (7) (a) C. Y. Xu, L. K. Li, Y. P. Wang, Q. Q. Guo, X. J. Wang, H. W. Hou, Y. T. Fan, *Cryst. Growth Des.*, 2011, **11**, 4667. (b) C. Y. Xu, Q. Q. Guo, X. J. Wang, H. W. Hou, Y. T. Fan, *Cryst. Growth Des.*, 2011, **11**, 1869. (c) L. Liu, Y. H. Liu, D. Q. Wu, H. W. Hou, Y. T. Fan, *Inorg. Chim. Acta.*, 2012, **391**, 66. (d) L. Liu, C. Huang, Z. C. Wang, D. Q. Wu, H. W. Hou, Y. T. Fan, *CrystEngComm*, 2013, **15**, 7095. (e) Q. Q. Guo, C. Y. Xu, B. Zhao, Y. Y. Jia, H. W. Hou, Y. T. Fan, *Cryst. Growth Des.*, 2012, **12**, 5439.
- (8) (a) E. Q. Gao, Z. M. Wang, C. S. Liao, C. H. Yan, *New J. Chem.*, 2002, **26**, 1096. (b) K. O. Ashiry, Y.-H. Zhao, K.-Z. Shao, Z.-M. Su, Y.-M. Fu, X.-R. Hao, *Inorg. Chem. Commun.*, 2008, **11**, 1181. (c) J. Y. Hu, J. P. Li, J. A. Zhao, H. W. Hou, Y. T. Fan, *Inorg. Chim. Acta.*, 2009, **362**, 5023.
- (9) (a) H. Kim, M. Y. P. Suh, *Inorg. Chem.*, 2005, **44**, 810. (b) Y. Qiu, H. Deng, S. Yang, J. Mou, C. Daiguebonne, N. Kerbellec, O. Guillou, S. R. Batten, *Inorg. Chem.*, 2009, **48**, 4158.
- (10) (a) J. Lv, J. X. Lin, X. L. Zhao, R. Cao, *Chem. Commun.*, 2012, **48**, 669. (b) B. Liu, Z. T. Yu, J. Yang, H. Wu, Y. Y. Liu, J. F. Ma, *Inorg. Chem.*, 2011, **50**, 8967. (c) P. P. Zhang, J. Peng, H. J. Pang, J. Q. Sha, M. Zhu, D. D. Wang, M. G. Liu, Z.-M. Su, *Cryst. Growth Des.*, 2011, **11**, 2736. (d) H. X. Li, X. Y. Zhang, Y. N. Huo, J. Zhu, *Environ. Sci. Technol.*, 2007, **41**, 4410.
- (11) (a) H. S. Lin, P. A. Maggard, *Inorg. Chem.*, 2008, **47**, 8044. (b) F. Wang, Z.-S. Liu, H. Yang, Y.-X. Tan, J. Zhang, *Angew. Chem., Int. Ed.*, 2011, **50**, 450. (c) Y.-Q. Chen, S.-J. Liu, Y.-W. Li, G.-R. Li, K.-H. He, Y.-K. Qu, T.-L. Hu, X.-H. Bu, *Cryst. Growth Des.*, 2012, **12**, 5426. (d) L. L. Wen, J. B. Zhao, K. L. Lv, Y. H. Wu, K. J. Deng, X. K. Leng, and D. F. Li, *Cryst. Growth Des.*, 2012, **12**, 1603. (e) J. R. Li, Y. Tao, Q. Yu, X. H. Bu, H. Sakamoto, S. Kitagawa, *Chem. Eur. J.*, 2008, **14**, 2771.
- (12) (a) J. Guo, J.-F. Ma, J.-J. Li, J. Yang, and S.-X. Xing, *Cryst. Growth Des.*, 2012, **12**, 6074. (b) W.-Q. Kan, B. Liu, J. Yang, Y.-Y. Liu, and J.-F. Ma, *Cryst. Growth Des.*, 2012, **12**, 2288. (c) X.-L. Wang, J. Luan, F.-F. Sui, H.-Y. Lin, G.-C. Liu, and C. Xu, *Cryst. Growth Des.*, 2013, **13**, 3561. (d) J.-S. Hu, Y.-J. Shang, X.-Q. Yao, L. Qin, Y.-Z. Li, Z.-J. Guo, H.-G. Zheng, and Z.-L. Xue, *Cryst. Growth Des.*, 2010, **10**, 4135. (e) X.-L. Wang, Q. Gao, A.-X. Tian, and G.-C. Liu, *Cryst. Growth Des.*, 2012, **12**, 2346.
- (13) (a) X. Wang, M.-M. Zhang, X.-L. Hao, Y.-H. Wang, Y. Wei, F.-S. Liang, L.-J. Xu, and Y.-G. Li, *Cryst. Growth Des.*, 2013, **13**, 3454. (b) T. Wen, D.-X. Zhang, J. Liu, R. Lin and J. Zhang, *Chem. Commun.*, 2013, **49**, 5660. (c) Q. Wu, W.-L. Chen, D. Liu, C. Liang, Y.-G. Li, S.-W. Lin and E. B. Wang, *Dalton Trans.*, 2011, **40**, 56. (d) Y. Hu, F. Luo, and F. F. Dong, *Chem. Commun.*, 2011, **47**, 761. (e) Y. Q. Chen, G. R. Li, Y. K. Qu, Y. H. Zhang, K. H. He, Q. Gao, X. H. Bu, *Cryst. Growth Des.*, 2013, **13**, 901.
- (14) Y. Gong, P.-G. Jiang, Y.-X. Wang, T. Wu and J.-H. Lin, *Dalton Trans.*, 2013, **42**, 7196.
- (15) (a) X.-L. Wang, J.-J. Huang, L.-L. Liu, G.-C. Liu, H.-Y. Lin, J.-W. Zhang, N.-L. Chen, Y. Qu, *CrystEngComm*, 2013, **15**, 1960. (b) H.-X. Yang, T.-F. Liu, M.-N. Cao, H.-F. Li, S.-Y. Gao, R. Cao, *Chem. Commun.*, 2010, **46**, 2429.
- (16) (a) R. Bronisz, *Inorg. Chem.*, 2005, **44**, 4463. (b) C. B. Aakeroy, J. Desper, B. Leonard, J. F. Urbina, *Cryst. Growth Des.*, 2005, **5**, 865.
- (17) G. M. Sheldrick, *Acta Crystallogr. A*, 2008, **64**, 112.
- (18) (a) L. Luo, K. Chen, Q. Liu, Y. Lu, T.-A. Okamura, G. C. Lv, Y. Zhao and W. Y. Sun, *Cryst. Growth Des.*, 2013, **13**, 2312. (b) T. L. Hu, R. Q. Zou, J. R. Li and X. H. Bu, *Dalton Trans.*, 2008, **10**, 1302. (c) X. Y. Lu, J. W. Ye, W. Li, W. T. Gong, L. J. Yang, Y. Lin and G. L. Ning, *CrystEngComm*, 2012, **14**, 1337.
- (19) (a) Q. G. Zhai, C. Z. Lu, X. Y. Wu, S. R. Batten, *Cryst. Growth Des.*, 2007, **11**, 2332. (b) D. K. Cao, Y. Z. Li, and L. M. Zhang, *Inorg. Chem.*, 2005, **44**, 2984.
- (20) (a) B. Liu, Y. C. Qiu, G. Peng, L. Ma, L. M. Jin, J. B. Cai, and H. Deng, *Inorg. Chem. Commun.*, 2009, **12**, 1200. (b) Y. Chen, V. Lykourinou, C. Vetroville, T. Hoang, L.-J. Ming, R. W. Larsen and S. Ma, *J. Am. Chem. Soc.*, 2012, **134**, 13188. (c) M. A. Braverman, R. L. LaDuca, *Cryst. Growth Des.*, 2007, **7**, 2343. (d) O. M. Yaghi, M. O'Keeffe, N. W. Ockwig, H. K. Chae, M. Eddaoudi, J. Kim, *Nature*, 2003, **423**, 705.
- (21) (a) Z. Q. Yu, M. Pan, J. J. Jiang, Z. M. Liu and C. Y. Su, *Cryst. Growth Des.*, 2012, **12**, 2389. (b) H. Y. Bai, J. F. Ma, J. Yang, Y. Y. Liu, H. Wu, J. C. Ma, *Cryst. Growth Des.*, 2010, **10**, 995.
- (22) (a) D. Sun, N. Zhang, R. B. Huang, L. S. Zheng, *Cryst. Growth Des.*, 2010, **10**, 3699. (b) S. S. Chen, R. Qiao, L. Q. Sheng, Y. Zhao, S. Yang, M. M. Chen, Z. D. Liu and D. H. Wang, *CrystEngComm*, 2013, **15**, 5713; (c) Q. R. Fang, G. S. Zhu, M. Xue, J. Y. Sun, F. X. Sun, S. L. Qiu, *Inorg. Chem.*, 2006, **45**, 3582. (d) J. Xu, Z. R. Pan, T. W. Wang, Y. Z. Li, Z. J. Guo, S. R. Batten and H. G. Zheng, *CrystEngComm*, 2010, **12**, 612.
- (23) P. Du, Y. Yang, J. Yang, Y.-Y. Liu, W.-Q. Kan and J.-F. Ma, *CrystEngComm*, 2013, **15**, 6986.